Implementation of Cavity Squeezing of a Collective Atomic Spin

Ian D. Leroux, Monika H. Schleier-Smith, and Vladan Vuletić

Department of Physics, MIT-Harvard Center for Ultracold Atoms and Research Laboratory of Electronics, Massachusetts Institute of Technology, Cambridge, Massachusetts 02139, USA

(Received 6 November 2009; published 17 February 2010)

We squeeze unconditionally the collective spin of a dilute ensemble of laser-cooled ^{87}Rb atoms using their interaction with a driven optical resonator. The shape and size of the resulting spin uncertainty region are well described by a simple analytical model [M. H. Schleier-Smith, I. D. Leroux, and V. Vuletić, arXiv:0911.3936 [Phys. Rev. A (to be published)]] through 2 orders of magnitude in the effective interaction strength, without free parameters. We deterministically generate states with up to 5.6(6) dB of metrologically relevant spin squeezing on the canonical ^{87}Rb hyperfine clock transition.

DOI: 10.1103/PhysRevLett.104.073602 PACS numbers: 42.50.Dv, 06.20.−f, 32.80.Qk, 42.50.Lc

Squeezed spin states [1–6], where a component of the total angular momentum of an ensemble of spins has less uncertainty [7,8] than is possible without quantum mechanical correlations [9–12], attract interest for both fundamental and practical reasons. Fundamentally, they allow the study of many-body entanglement but retain a simple description in terms of a single collective angular-momentum variable [4,5]. Practically, they may be a means to overcome the projection noise limit on precision [2,3,13,14]. Spin squeezing has been demonstrated using entanglement of ions via their shared motional modes [9], repulsive interactions in a Bose-Einstein condensate [10], or partial projection by measurement [11,12].

In a companion paper [15] we propose a cavity feedback method for deterministic production of squeezed spin states using light-mediated interactions between distant atoms in an optical resonator. This approach generates spin dynamics similar to those of the one-axis twisting Hamiltonian $H \propto S_z^2$ in the original proposal of Kitagawa and Ueda [1]. Cavity squeezing scales to a much higher particle number than direct manipulation of ions [9] (but see Ref. [16] for a potentially scalable approach) and employs dilute ensembles rather than dense condensates of interacting atoms [10]. Unlike measurement-based squeezing [11,12], it unconditionally produces a known squeezed state independent of detector performance.

Here we implement cavity squeezing for the canonical $|F = 1, m_F = 0\rangle \leftrightarrow |F = 2, m_F = 0\rangle$ hyperfine clock transition in ^{87}Rb atoms, achieving a 5.6(6) dB improvement in signal-to-noise ratio [2,3]. To our knowledge, this is the largest such improvement to date. Moreover, the shape and orientation of the uncertainty regions we observe agree with a straightforward analytical model [15], without free parameters, over 2 orders of magnitude in effective interaction strength.

Our scheme, similar in spirit to the proposal of Ref. [17], relies on the repeated interaction of the atomic ensemble with light circulating in an optical resonator, as illustrated in Fig. 1. We label the two relevant eigenstates (clock states) of each one of N_0 atoms as the spin-up and spin-down states of a spin-1/2 $\boldsymbol{s}_i$, and define a total spin $\boldsymbol{S} = \sum_i \boldsymbol{s}_i$. Its z component corresponds to the population difference between clock states, and its azimuthal angle corresponds to their relative phase. For a given total spin magnitude $S = |\boldsymbol{S}| \leq S_0 = N_0/2$ and a given permutation symmetry of the ensemble, the set of possible collective states forms a Bloch sphere.

The coupling of the atoms to the resonator manifests itself both as a differential light shift of the clock states which causes the $\boldsymbol{s}_i$ to precess about the $\hat{z}$ axis and as a modified index of refraction which shifts the cavity resonance frequency. If a resonator mode is tuned halfway between the optical transition frequencies for the two clock

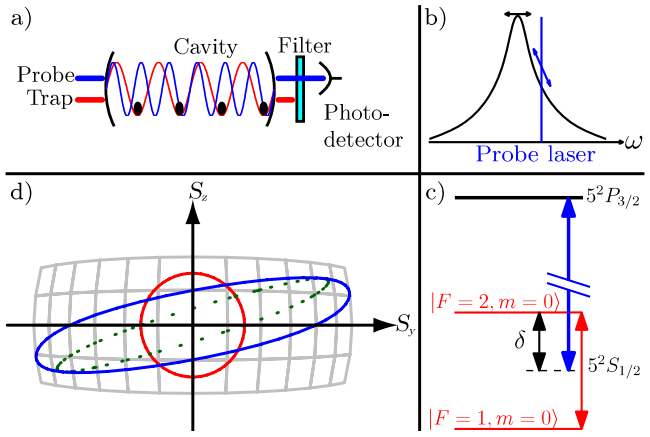

FIG. 1 (color online). Cavity squeezing [15]. (a) The atoms are trapped in a standing-wave dipole trap inside an optical resonator. (b) The probe laser is detuned from cavity resonance by half a linewidth, so that atom-induced shifts of the cavity frequency change the transmitted power. (c) The cavity is tuned halfway between the optical transition frequencies for the two clock states. (d) The S_z-dependent light shift shears the circular uncertainty region of the initial coherent spin state (red circle) into an ellipse (dotted). Photon shot noise causes phase broadening that increases the ellipse area (solid). The illustration is for a modest shearing $Q = 3$ (see text).

states [Fig. 1(c)], the atomic index of refraction produces opposite frequency shifts of the mode for atoms in each of the states, yielding a net shift $\Delta\omega_r/\kappa = \phi_1 S_z/2 \ll 1$ proportional to the population difference $2S_z$. Here κ is the linewidth of the resonator and ϕ_1 is the spin precession angle per photon transmitted through the resonator. The resonator is driven by a probe laser with fixed incident power at a detuning $\kappa/2$ so that this mode frequency shift changes the average number of photons transmitted by $\Delta p = p_0\phi_1 S_z$ from its value p_0 in the absence of atoms. As the intracavity power is S_z-dependent, so is the light shift, which produces a precession of each spin through an angle $\phi(S_z) = QS_z/S_0$. The state of each atom now depends, through S_z, on that of all other atoms in the ensemble. The shearing strength $Q = S_0 p_0 \phi_1^2$ is a dimensionless measure of the light-mediated interaction strength. In particular, a coherent spin state prepared on the equator of the Bloch sphere (an uncorrelated state with $\langle \boldsymbol{S}\rangle = S\hat{\boldsymbol{x}}$ and $\Delta S_y^2 = \Delta S_z^2 = S/2$) has its circular uncertainty region sheared into an ellipse with a shortened minor axis [Fig. 1(d)] [15].

Two fundamental decoherence mechanisms counteract the unitary evolution which squeezes the spin uncertainty. The first is photon shot noise: the intracavity light field, driven by a coherent input and decaying via the cavity mirrors, is not in a photon number state and produces an uncertain light shift. This uncertainty leads to irreversible phase broadening $\Delta\phi^2 = p_0\phi_1^2/2 = Q/(2S_0)$. The squeezed variance, which would lessen as Q^{-2} if the dynamics preserved the area of the uncertainty region, therefore only decreases as Q^{-1} [15].

The second decoherence process is photon scattering into free space. Scattered photons that reveal the state of individual atoms spoil the ensemble's coherence, while Raman scattering, which changes the atoms' internal state at random, increases the spin variance [18]. In our system, Rayleigh scattering occurs at the same rate for the two clock states, does not reveal the atomic state, and so does not harm the coherence [19]. At most, 2.3% of the atoms undergo Raman scattering for our parameters, causing added noise and decoherence [18] much smaller than those from technical sources.

Finally, the coherent shearing action ceases to reduce the minimum spin variance once the uncertainty region becomes elongated enough that the curved geometry of the Bloch sphere becomes important [1]. Such curvature effects are visible in our data for large values of the shearing strength Q.

For the experimental demonstration, up to $N_{\mathrm{tot}} = 5 \times 10^4$ atoms of ^{87}Rb (with excited-state decay rate $\Gamma = 2\pi \times 6.065$ MHz) are confined in a standing-wave optical dipole trap inside a Fabry-Pérot resonator of linewidth $\kappa = 2\pi \times 1.01(3)$ MHz. Details of the apparatus are given in Ref. [11]. The atoms are coupled to the resonator with a position-dependent dimensionless cooperativity $\eta(\boldsymbol{r}) = 4g(\boldsymbol{r})^2/\kappa\Gamma$, where $2g(\boldsymbol{r})$ is the vacuum Rabi frequency [20]. We define an effective cooperativity η and atom number N_0 for an equivalent uniformly coupled system so that the spin variance of a coherent spin state, measured via the resonator frequency shift, is $\Delta S_z^2 = S_0/2 = N_0/4$. The effective quantities must satisfy $N_0\eta = N_{\mathrm{tot}}\langle\eta(\boldsymbol{r})\rangle_e$, where $\langle\rangle_e$ denotes an average over the ensemble, in order to reproduce the observed average frequency shift. Reproducing the projection-noise-induced variance of the cavity shift requires $N_0\eta^2 = N_{\mathrm{tot}}\langle\eta(\boldsymbol{r})^2\rangle_e$. These two constraints impose the definitions $\eta = \langle\eta(\boldsymbol{r})^2\rangle_e/\langle\eta(\boldsymbol{r})\rangle_e = 0.139(5)$ and $N_0 = N_{\mathrm{tot}}\langle\eta\rangle_e/\eta$. The effective total spin has $S_z = (N_2 - N_1)/2$, where $N_{1,2}$ are the analogously defined effective populations of the clock states.

We prepare an initial coherent spin state by optically pumping the atoms into $|F = 1, m_F = 0\rangle$ ($\langle \boldsymbol{S}\rangle = -S_0\hat{\boldsymbol{z}}$) and applying a microwave $\pi/2$ pulse to yield $\langle \boldsymbol{S}\rangle = S_0\hat{\boldsymbol{x}}$. The squeezing is performed by two pulses of 780 nm light detuned 3.18(1) GHz to the blue of the $|5^2S_{1/2}, F = 2\rangle \leftrightarrow |5^2P_{3/2}, F' = 3\rangle$ transition and 500 kHz to the blue of the cavity resonance. This yields a single-photon phase shift $\phi_1 = (2/3)\eta\Gamma/\delta = 171(6)\ \mu$rad, where $\delta = 2\pi \times 3.29$ GHz is the effective detuning from the $5^2P_{3/2}$ manifold with oscillator strength 2/3. Between the two optical pulses, each of which lasts 50 μs $\gg \kappa^{-1}$ and contains up to $\sim 10^5$ photons, is a composite [SCROFULOUS (short composite rotation for undoing length over and under shoot) [21]] microwave π pulse, forming a spin echo sequence. The spin echo cancels the spatially inhomogeneous phase shift caused by the p_0 photons transmitted on average through the resonator but preserves the shearing effect. We measure S_z using this same sequence but with stronger optical pulses, with 10^6 photons transmitted on average. The transmitted fraction of these pulses, measured on an avalanche photodiode, reveals the cavity resonance frequency shift and hence S_z [11].

We observe the shearing by rotating the state through an angle α with a microwave pulse about the axis of its mean spin vector and recording the variance ΔS_α^2 of a subsequent measurement of $S_z|_\alpha$ over a series of 100 identical preparations. The measured variance is normalized to projection noise $\sigma^2(\alpha) = 2\Delta S_\alpha^2/S_0$ where S_0 is determined from our atom number calibration, based on a first-principles calculation using accurately measured cavity parameters [11]. The inset of Fig. 2 shows the observed ΔS_z^2 of the initial spin state as a function of S_0, as well as the calculated projection noise limit.

Typical data of ΔS_α^2 are displayed in Fig. 2. As the state is rotated the variance dips below projection noise as the minor axis of the ellipse is aligned with $\hat{\boldsymbol{z}}$ and then increases beyond it as the major axis in turn rotates towards $\hat{\boldsymbol{z}}$. The variation of ΔS_α^2 with angle is sinusoidal with a period π, as it must be for any distribution of S_y-S_z fluctuations. We record such curves over a range of photon numbers, corresponding to increasing shearing strength Q, keeping the effective atom number constant at $2S_0 \approx 3.2 \times 10^4$. We compare the fitted phase and minimum

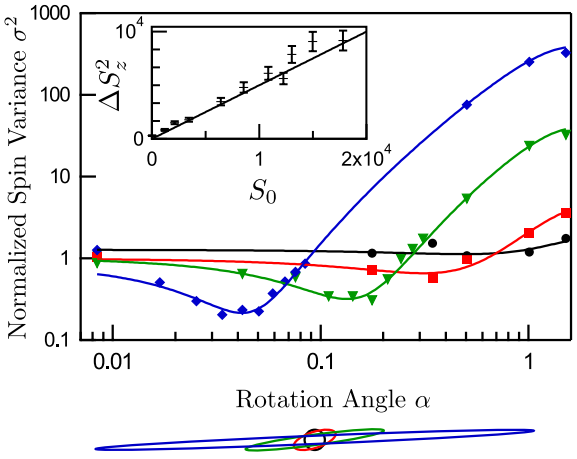

FIG. 2 (color online). Normalized variance σ^2 as a function of rotation angle α about the mean spin direction for states prepared with shearing $Q = 0$ (black circles), $Q = 1.2$ (red squares), $Q = 7.7$ (green triangles), and $Q = 30.7$ (blue diamonds). The curves are cosine fits. Statistical error bars are comparable to the symbol size. The shapes of the corresponding uncertainty regions are illustrated below the plot. Inset: Observed variance ΔS_z^2 of the initial state as a function of S_0. The line is the projection noise limit as determined from cavity parameters.

and maximum variance of each sinusoid to the predictions of our model [15], briefly described below.

Neglecting scattering, the initial S_z distribution with $\Delta S_z^2 = S_0/2$ is unaffected by the shearing, while the S_y variance is modified [15]

$$\Delta S_y^2 = \frac{S^2}{2} + \frac{S_0}{4} - \left(\frac{S^2}{2} - \frac{S_0}{4}\right)\left(1 - \frac{\gamma Q}{S_0}\right)e^{-\xi^2 Q^2/S_0}, \quad (1)$$

and an S_y-S_z correlation is introduced

$$W = \langle S_y S_z + S_z S_y \rangle = \xi Q S e^{-\xi^2 Q^2/(4S_0)}. \quad (2)$$

The expressions given here are approximations to those of the companion theory paper [15], with which they agree to within 0.01% for our parameters. They include additional correction factors ξ, γ, and S/S_0 to account for technical imperfections. $\xi = (d\mathcal{L}/d\omega_p)\kappa/(2\mathcal{L})$ is the logarithmic derivative of the Lorentzian resonator transmission $\mathcal{L}$ with respect to fractional probe detuning ω_p/κ. Ideally, $\omega_p = \kappa/2$ and $\xi = 1$ exactly. As we do not maintain precisely this detuning, $0.97 \leq \xi \leq 1$ for the data presented here. The variance of the intracavity probe power in the absence of atoms, expressed as a multiple of photon shot noise, is $\gamma = 1 + 2\Delta p_f^2/p_0 = 1 + p_0/(8 \times 10^4) = 1 + Q/37$, where Δp_f^2 is the additional variance in the transmitted photon number caused by independently determined fractional light noise. Finally, dephasing reduces the effective radius of the Bloch sphere from S_0 to S, measured from the envelope amplitude of a Rabi nutation curve. For modest shearing $Q < 20$ we maintain a Bloch sphere radius $S > 0.80S_0$, but when Q reaches 200 the radius is reduced to $S = 0.48S_0$.

Equations (1) and (2) together yield a prediction for the observed normalized variance:

$$\sigma^2(\alpha) = \frac{1}{S_0}[V_+ - A\cos(2\alpha - 2\alpha_0)] + \sigma_{\mathrm{ro}}^2, \quad (3)$$

where $V_\pm = \Delta S_y^2 \pm \Delta S_z^2$, $A = \sqrt{V_-^2 + W^2}$, and the rotation angle which minimizes the variance is $\tan(2\alpha_0) = W/V_-$. The additional variance of our imperfect readout $\sigma_{\mathrm{ro}}^2 = 0.13$ is determined by comparing successive measurements of the same state as in Ref. [11].

Figure 3 shows the predictions of maximum and minimum variance $\sigma^2_{\substack{\mathrm{max}\\\mathrm{min}}} = (V_+ \pm A)/S_0 + \sigma_{\mathrm{ro}}^2$ and orientation α_0 as black lines, together with the data points extracted from the cosine fits. It is remarkable that a simple analytical model, without free parameters, provides good predictions of the shape, area, and orientation of the uncertainty region for values of the shearing strength Q that span a factor of 200. Note the increase of the minimum variance σ_{min}^2 for large shearing as the curvature of the Bloch sphere becomes important. For comparison, Fig. 3 also includes the model predictions without technical corrections ($S = S_0$, $\gamma = \xi = 1$, $\sigma_{\mathrm{ro}}^2 = 0$) as blue dashed curves. The maximal noise σ_{max}^2 and the ellipse angle α_0, dominated by the shearing-induced broadening along $\hat{\mathbf{y}}$, are insensitive to technical effects, but the minimum variance σ_{min}^2 is strongly affected by readout noise σ_{ro}^2. This noise is due to a combination of finite quantum efficiency and avalanche noise of the photodetector together with Raman

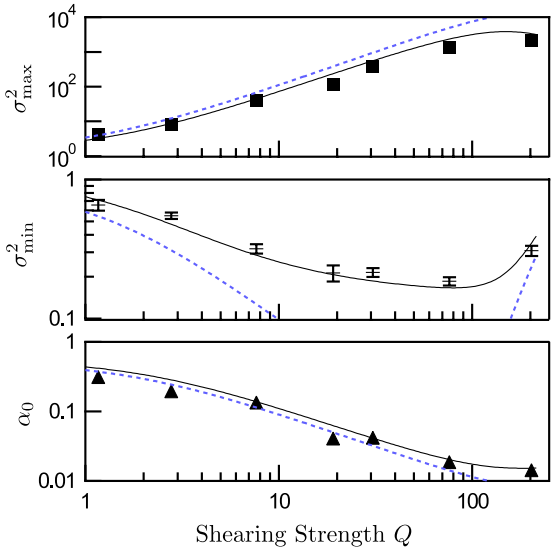

FIG. 3 (color online). σ_{max}^2 (top panel) is the normalized maximum variance, σ_{min}^2 (middle panel) the normalized minimum variance, and α_0 (bottom panel) the rotation angle for minimum variance for each measured ellipse as a function of shearing strength Q. Statistical error bars are given for σ_{min}^2, and are smaller than the symbols for σ_{max}^2 and α_0. The blue dashed curves are theoretical predictions for an ideal system, while the black lines are predictions including separately measured technical imperfections. Shearing was varied by adjusting the photon number $p_0 \approx 2200 \times Q$.

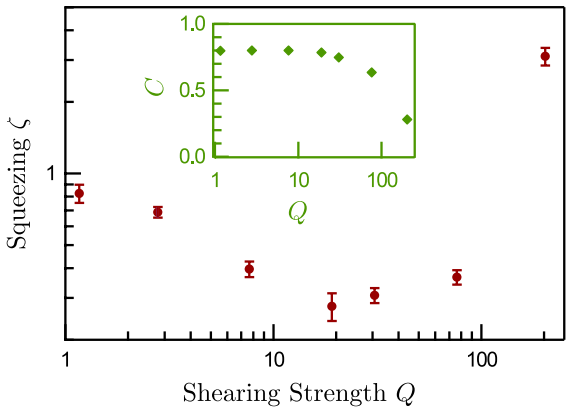

FIG. 4 (color online). Metrologically relevant squeezing ζ (red solid circles) and signal contrast C (green diamonds, inset) as a function of shearing strength Q.

scattering which limits the number of photons in the readout measurement. It could be suppressed by using a different photodetector to remove the avalanche noise and by performing the readout near-detuned to a cycling transition to suppress Raman scattering [18].

To determine whether the reduced spin noise σ^2_{min} allows a gain in spectroscopic precision, we must establish a signal-to-noise ratio by comparing it to the mean spin signal $|\langle \boldsymbol{S}\rangle|$ [2]. $|\langle \boldsymbol{S}\rangle|$ is reduced below S_0 by dephasing, which shortens the Bloch vector, and by shot-to-shot phase fluctuations which reduce the average projection of $\boldsymbol{S}$ along its mean direction. We specify the signal strength by a contrast $C = |\langle \boldsymbol{S}\rangle|/S_0$, measured from the mean amplitude of Rabi oscillations with the sheared state as input, and plotted in the inset of Fig. 4. The signal contrast in the absence of squeezing light $C_{\mathrm{in}} = 0.80$ is limited by dephasing from the lock light used to stabilize the cavity length [11].

Figure 4 shows the metrological squeezing parameter [2] $\zeta = 2|\langle \boldsymbol{S}\rangle|_{\mathrm{in}}/(|\langle \boldsymbol{S}\rangle|^2/\Delta S_z^2) = \sigma^2_{\mathrm{min}} C_{\mathrm{in}}/C^2$, which compares the squared signal-to-noise ratio for an ideal projection-noise-limited measurement using the initial spin signal $|\langle \boldsymbol{S}\rangle|_{\mathrm{in}} = C_{\mathrm{in}} S_0$ to that for the minimum observed variance and corresponding signal $|\langle \boldsymbol{S}\rangle|$. $\zeta < 1$ indicates an improvement in signal-to-noise ratio unattainable without entanglement [2]. For $S_0 = 1.6 \times 10^4$ and $p_0 = 4.1 \times 10^4$ ($Q = 19$), we reduce the spin noise by a factor $\sigma^2_{\mathrm{min}} = -6.7(6)$ dB. At this photon number our contrast is $C = 0.78(2)$, so that we demonstrate a $\zeta^{-1} = 5.6(6)$ dB improvement in potential measurement precision over that of the initial uncorrelated state.

By subtracting our independently measured readout noise σ^2_{ro} from σ^2_{min}, we infer that states prepared by a shearing $Q = 19$ have an intrinsic spin variance that is a full 10(1) dB below the projection noise limit. However, it is the observed and not the intrinsic variance that determines the precision of a spectroscopic measurement, and we use the former in calculating the spin noise reduction and the squeezing ζ.

In conclusion, we have demonstrated a method for deterministically generating squeezed states using switchable light-mediated interactions in a dilute ensemble of otherwise noninteracting atoms. Our model predicts the size and shape of the uncertainty region when technical effects are included. We hope to observe states with substantially lower spin noise by improving our readout, and to demonstrate their use in an atomic clock.

This work was supported in part by the NSF, DARPA, and the NSF Center for Ultracold Atoms. M. H. S. acknowledges support from the Hertz Foundation and NSF. I. D. L. acknowledges support from NSERC.

[1] M. Kitagawa and M. Ueda, Phys. Rev. A **47**, 5138 (1993).
[2] D. J. Wineland, J. J. Bollinger, W. M. Itano, F. L. Moore, and D. J. Heinzen, Phys. Rev. A **46**, R6797 (1992).
[3] D. J. Wineland, J. J. Bollinger, W. M. Itano, and D. J. Heinzen, Phys. Rev. A **50**, 67 (1994).
[4] A. S. Sørensen and K. Mølmer, Phys. Rev. Lett. **86**, 4431 (2001).
[5] A. Sørensen, L.-M. Duan, J. I. Cirac, and P. Zoller, Nature (London) **409**, 63 (2001).
[6] A. Kuzmich, N. P. Bigelow, and L. Mandel, Europhys. Lett. **42**, 481 (1998).
[7] A. Kuzmich, L. Mandel, and N. P. Bigelow, Phys. Rev. Lett. **85**, 1594 (2000).
[8] T. Takano, M. Fuyama, R. Namiki, and Y. Takahashi, Phys. Rev. Lett. **102**, 033601 (2009).
[9] V. Meyer, M. A. Rowe, D. Kielpinski, C. A. Sackett, W. M. Itano, C. Monroe, and D. J. Wineland, Phys. Rev. Lett. **86**, 5870 (2001).
[10] J. Estéve, C. Gross, A. Weller, S. Giovanazzi, and M. K. Oberthaler, Nature (London) **455**, 1216 (2008).
[11] M. H. Schleier-Smith, I. D. Leroux, and V. Vuletić, arXiv:0810.2582 [Phys. Rev. Lett. (to be published)].
[12] J. Appel, P. J. Windpassinger, D. Oblak, U. B. Hoff, N. Kjærgaard, and E. S. Polzik, Proc. Natl. Acad. Sci. U.S.A. **106**, 10 960 (2009).
[13] A. André, A. S. Sørensen, and M. D. Lukin, Phys. Rev. Lett. **92**, 230801 (2004).
[14] G. Santarelli, P. Laurent, P. Lemonde, A. Clairon, A. G. Mann, S. Chang, A. N. Luiten, and C. Salomon, Phys. Rev. Lett. **82**, 4619 (1999).
[15] M. H. Schleier-Smith, I. D. Leroux, and V. Vuletić, arXiv:0911.3936 [Phys. Rev. A (to be published)].
[16] D. Leibfried, M. D. Barrett, T. Schaetz, J. Britton, J. Chiaverini, W. M. Itano, J. D. Jost, C. Langer, and D. J. Wineland, Science **304**, 1476 (2004).
[17] M. Takeuchi, S. Ichihara, T. Takano, M. Kumakura, T. Yabuzaki, and Y. Takahashi, Phys. Rev. Lett. **94**, 023003 (2005).
[18] M. Saffman, D. Oblak, J. Appel, and E. S. Polzik, Phys. Rev. A **79**, 023831 (2009).
[19] R. Ozeri *et al.*, Phys. Rev. Lett. **95**, 030403 (2005).
[20] H. J. Kimble, Phys. Scr. **T76**, 127 (1998).
[21] H. K. Cummins, G. Llewellyn, and J. A. Jones, Phys. Rev. A **67**, 042308 (2003).